Journal of Engineering Physics and Thermophysics, Vol. 75, No. 3, 2002

NUMERICAL MODELING OF THE THREE-DIMENSIONAL UNSTEADY CONVECTION OF A SILICON MELT IN A VESSEL TYPICAL OF CZOCHRALSKI-METHOD APPARATUSES

N. G. Ivanov and E. M. Smirnov

UDC 532.516:536.25

Calculations of the quasiperiodic and stochastic regimes of three-dimensional convection of a silicon melt (Pr = 0.015) have been performed for a rotating vessel whose complicated shape is typical of crucibles used in growing crystals by the Czochralski method. A large set of data on the structure of the convection and the spectral composition of pulsations has been obtained. The influence of the rotation of a crystal and a crucible on the convection and the thermal state of a melt has been investigated.

1. Convection of a melt in the case of both the predominant influence of buoyancy forces and the effects of Coriolis forces and buoyancy forces comparable in significance plays a decisive role in growing semiconductor crystals by the Czochralski method [1]. The basis for this method is provided by the process of crystallization of a semiconductor on a cooled seed which is pulled, at a certain speed, upward from a melt placed in a heated crucible. Experimental investigations point to a multimode unsteady and frequently turbulent character of the convection under conditions characteristic of Czochralski-method apparatuses [2, 3]. Three-dimensional pulsations of the melt can exert a substantial influence on the quality of the crystal produced, in particular, by changing the position and shape of the crystal/melt interface and determining the content of the impurities in the crystal.

With increase in computer powers, experimental investigations of three-dimensional effects in motion of a silicon melt have begun to be supplemented with the results of numerical modeling in a three-dimensional formulation (see [5] and the references therein). It must be noted that because of the opacity of semiconductor melts and a number of other complicating circumstances, virtually the entire experimental information is confined at present to the results of temperature measurements at individual points, which makes it impossible to safely judge the flow structure. In growing crystals by the Czochralski method, the motion of a melt has been modeled so far for cylindrical regions, as a rule, on condition that the temperature of cold and hot walls is distributed uniformly [6, 7]. It does not seem possible to extend the results obtained directly to the flow in an actual crucible having a complex geometric shape and a nonuniform wall temperature. Therefore, in parallel to investigations of a fundamental character carried out for vessels of simplified geometry, one should also accumulate calculated data on the properties of convection which develops in vessels with a geometry typical of Czochralski-method crucibles for a wall-temperature distribution typical of the technology.

2. Let us consider the convection of a melt in a rotating vessel (crucible) with the geometry shown in Fig. 1. The free surface of the melt will be set flat for $r > R_m$ and curved in accordance with typical parameters of a meniscus for $R_s \le r \le R_m$. The central part of the upper boundary ($r < R_s$) will be interpreted as the crystal/melt interface. Here and in what follows, we take, as the characteristic length, the vessel height H determined as the distance from the lower point of the bottom to a plane passing through the uncurved part of the free surface. The basic geometric relations are as follows: $R_c : H = 1.74$, $R_m : H = 0.6$, and $R_s : H = 0.53$.

To describe the motion of the liquid we employ the system of unsteady three-dimensional equations of continuity, motion, and energy. The equations of motion are written in a coordinate system rotating together with the vessel at a constant angular velocity. The buoyancy effects in the gravity field and in the centrifugal-force field are taken into

St. Petersburg State Technical University, St. Petersburg, Russia; email: aerofmf@citadel.stu.neva.ru. Translated from Inzhenerno-Fizicheskii Zhurnal, Vol. 75, No. 3, pp. 63–69, May–June, 2002. Original article submitted July 11, 2001.

1062-0125/02/7503-0599$27.00

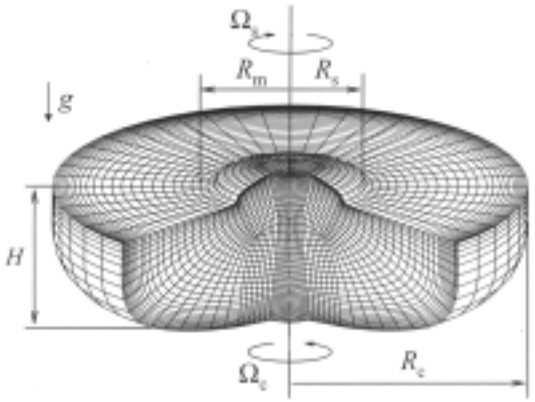

Fig. 1. Geometry of the vessel and the three-block computational scheme.

TABLE 1. Values of the Diagnostic Variables for the Considered Variants

Variant	Ra	Ra_Ω	Re_s	Ro
1	$5.9\cdot10^3$	$1.5\cdot10^2$	520	1.38
2	$6.6\cdot10^4$	$1.6\cdot10^3$	1732	1.38
3	$6.6\cdot10^4$	$1.6\cdot10^3$	0	1.38
4	$6.6\cdot10^4$	$6.6\cdot10^1$	1732	6.67

account in the Boussinesq approximation. With account taken of the above assumptions, the system of dimensionless equations which describe thermal convection can be represented in the form

$$\nabla\cdot\mathbf{V} = 0\,, \tag{1}$$

$$\frac{\partial\mathbf{V}}{\partial t} + (\mathbf{V}\cdot\nabla)\,\mathbf{V} = -\,\mathrm{grad}\,p^* + \frac{\sqrt{\mathrm{Pr}}}{\sqrt{\mathrm{Ra}}}\Delta\mathbf{V} - T\,\mathbf{e}_g - \frac{\mathrm{Ra}_\Omega}{\mathrm{Ra}}\frac{H^3}{R_c^3}\,Tr\,\mathbf{e}_r - \frac{2}{\mathrm{Ro}}\,(\mathbf{e}_\Omega\times\mathbf{V})\,, \tag{2}$$

$$\frac{\partial T}{\partial t} + (\mathbf{V}\cdot\nabla)\,T = \frac{1}{\sqrt{\mathrm{Pr}\,\mathrm{Ra}}}\Delta T\,. \tag{3}$$

The flow in the region for the specified geometry is determined by the following dimensionless parameters: the Prandtl number Pr, the Rayleigh number in the gravity field Ra and in the centrifugal-force field Ra_Ω, the Rossby number Ro, and the Reynolds number Re_s constructed from the rotational velocity of the central body.

All the calculations have been performed for the value Pr = 0.015 which is characteristic of the silicon melt. The values of the remaining diagnostic variables for the four variants presented are indicated in Table 1. Variants 1 and 2 differ in the values of the Rayleigh number. Consideration of variant 3 in comparison to variant 2 is aimed at studying the influence of rotation of a crystal, while passage to variant 4 is aimed at revealing a change in the character of the flow with substantial increase in the Rossby number. In the considered range of diagnostic variables, the buoyancy effects in the centrifugal-force field are much weaker than the effects caused by the gravity force ($\mathrm{Ra}_\Omega \ll \mathrm{Ra}$, see Table 1); therefore, we did not carry out additional calculations aimed at refining the influence of buoyancy effects in the centrifugal-force field.

For the velocity on the crucible walls, in formulating the problem for a coordinate system rotating together with the crucible, we specify the condition of zero speed while at the crystal/melt interface the velocity distribution corresponds to the relation $V = -(\Omega_s + \Omega_c)r$. The condition of absence of the tangential components of the friction stress is imposed on the free surface. The thermal boundary conditions are as follows: the normalized temperature is set equal to zero at the crystal/melt interface, the axisymmetric temperature distribution (typical of the technology of

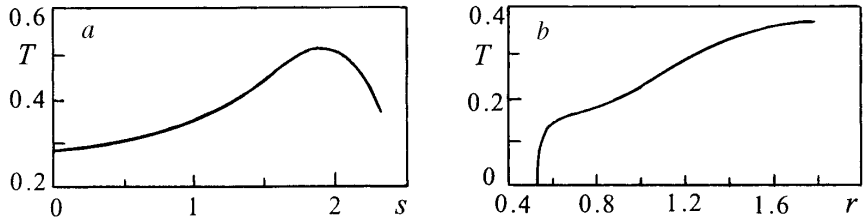

Fig. 2. Thermal boundary conditions on the vessel wall (a) and on the free surface (b).

crystal growth of the Czochralski method) with the characteristic maximum in the vicinity of the site of junction of the lateral surface of the walls and the lenticular bottom is specified on the vessel wall (see Fig. 2a), and the typical temperature distribution is also specified on the free surface (see Fig. 2b).

Comparison calculations in the axisymmetric formulation were carried out for a narrow sector; the conditions of rotational symmetry were specified on the lateral walls. To eliminate the problem of singularity in the vicinity of the axis of rotation we introduced a central body of radius 0.1 on whose surface we specified the condition of slip for velocity and the zero heat flux.

3. In the calculations, we employed the SINF software system developed at the Department of Hydroaerodynamics of the St. Petersburg State Technical University; this system makes it possible to calculate steady-state and unsteady flows developing in the general case in regions of complex geometry. The numerical method is based on the employment of multiblock structurized nonuniform grids matched with the boundaries of the flow region. The equations of motion are written relative to Cartesian velocity components. The implicit three-layered scheme of second order in physical time is realized to obtain unsteady solutions. Iterations on the new time layer are carried out by the artificial-compressibility method. On each iteration, we provide the exchange of the values of the calculated variables along the surfaces at which blocks of the computational grid are joined. The concept of an auxiliary virtual block is used, which creates the total transparency of interblock boundaries and preserves the conservative properties of a difference scheme. Discretization of the space operators of the equations of conservation is performed by the control-volume method of second order of accuracy. The values of the quantities sought are determined at the centers of the control volumes. Of the possibilities available in the software system to calculate convective terms, in the present work we have selected the QUICK upwind difference scheme [8].

Calculations in the three-dimensional formulation were carried out on a three-block grid with a total dimension of 35,712 cells with bunching toward solid walls and toward the free surface (see Fig. 1). The step of dimensionless time was taken to be 0.125 for variants 1–3 and 0.0625 in case 4. Here and in what follows, the time is normalized to the ratio H/V_b. In variant 1, we took the zero values of the relative velocities and the average value of the normalized temperature as the initial field, while in variants 2–4 we used the results of calculation for variant 1 as the initial fields. In all the cases the length of the samples obtained was from 200 to 300 time units; in constructing spectral characteristics, the initial portion with a length of 70 time units was omitted.

Calculations in the axisymmetric formulation were carried out with the use of a three-dimensional grid which consisted of two blocks whose dimension was 22×50 and 20×30 cells in the meridional section. The grid contained two cells in the azimuthal direction.

4. The calculation results for variants 1 and 2 enable us to understand the regularities of behavior of the melt for a comparatively low value of the Rossby number, which, however, is within the range characteristic of the technology of crystal growth by the Czochralski method. The flow structure under these conditions is illustrated by Fig. 3a and b, in which the instantaneous patterns of the velocity vectors in the vertical section are shown for variants 1 and 2 respectively. In Fig. 3a ($\mathrm{Ra} = 5.9 \cdot 10^3$), the subdivision of the flow into two zones, i.e., the subcrystal region characterized by intense motion directly under the central body and the descending central vortex and the peripheral region where the flow is strongly inhibited by rotation (characteristic velocities are hundredths of a fraction of the buoyancy velocity), is pronounced. This subdivision is also preserved for $\mathrm{Ra} = 6.6 \cdot 10^4$, although it becomes less pronounced (Fig. 3b). In this case, the flow in the subcrystal region is strongly complicated and one cannot single out the central vortex.

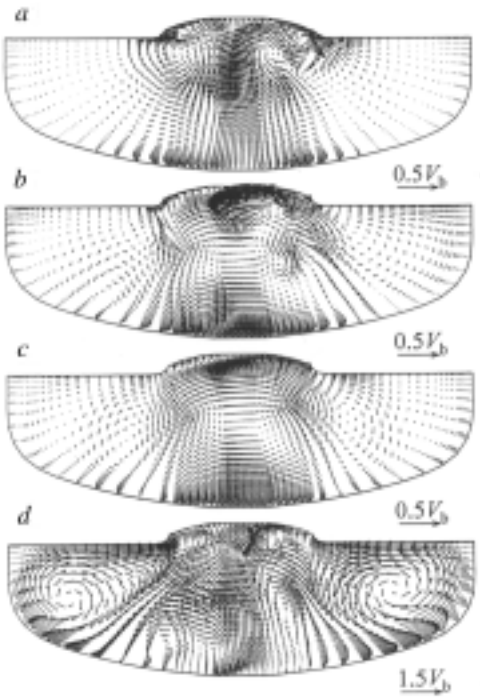

Fig. 3. Instantaneous velocity distributions in the vertical section: a–d) variants 1–4 respectively.

In the subcrystal region, one should in turn single out the layer adjacent to the crystal/melt interface where the liquid is scattered from the axis to the edges of the crystal owing to the faster rotation of the crystal than the rotation of the vessel. Because of this, subcrystal toroidal flow (clearly observed in Fig. 3a) is formed. With increase in the Rayleigh number the thickness of the region of the scattered liquid decreases and the degree of order of the subcrystal torus drops (Fig. 3b).

Despite the comparatively low values of the Rayleigh number in the considered regimes, convection of the melt is substantially unsteady and the axial symmetry is broken. The latter is illustrated in Fig. 4a and b, in which the instantaneous distributions of the vertical velocity in the horizontal section $z = 0.64$ are given for variants 1 and 2. When $\mathrm{Ra} = 5.9 \cdot 10^3$ the values of the velocity are low at the periphery of the vessel and the deviations from axial symmetry are weak. Closer to the central part of the vessel, approximately on the middle radius, vortex structures are formed which drift in the direction opposite to the direction of rotation of the vessel. Strong descending flow is observed in the vicinity of the axis. With increase in the Rayleigh number the structure of the flow is substantially complicated (Fig. 4b). We also note that the instantaneous temperature field remains axisymmetric, in practice, for the first variant and deviates appreciably from axial symmetry for the second variant, which can exert a substantial influence on the properties of the crystal produced.

Fluctuations of temperature at the monitoring point which is located at a distance of 0.1 from the axis of rotation (the vertical coordinate is equal to 0.9; it is also worthwhile to note that this point is found to be in the vicinity of the site of junction of the subcrystal torus and the descending axial vortex) are shown in Fig. 5a and b for the analyzed cases 1 and 2. Information is presented for the monitoring point rotating together with the vessel. When $\mathrm{Ra} = 5.9 \cdot 10^3$ the amplitude of temperature fluctuations is small: it is no more than two hundredths of the total difference. Nonetheless, the character of the fluctuations (Fig. 5a) enables us to infer that variant 1 should also be related to the chaotic regimes of flow. This is demonstrated by the results of spectral analysis presented in Fig. 6a for this value of the Rayleigh number. The principal maximum of the energy spectrum corresponds to the low-frequency modulation of fluctuations with a period of about 35 time units (see Fig. 5a). The second pronounced maximum of the energy spectrum corresponds to a control frequency of fluctuations of about 0.14; the maxima at the frequencies which are multiples of the control one ($f \approx 0.28$ and 0.42) are also present on the graph. On the whole, the spectrum corresponds to a flow in which regular and irregular components of fluctuations coexist.

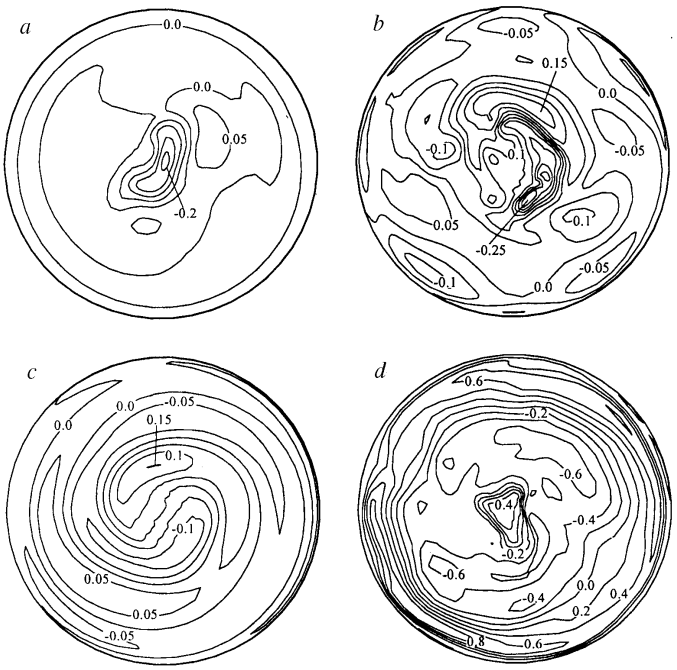

Fig. 4. Instantaneous distributions of the vertical velocity in the horizontal section $z = 0.64$: a–d) variants 1–4 respectively.

For variant 2 ($\mathrm{Ra} = 6.6 \cdot 10^4$) the amplitude of temperature fluctuations increases by about an order of magnitude as compared to the case considered earlier and attains nearly one tenth of the difference (Fig. 5b); thus, significant intensification of three-dimensional pulsations occurs. The pronounced principal maximum of the energy spectrum is at a frequency of $f \approx 0.12$ (Fig. 6b).

5. Let us now direct our attention to the results of calculations which have been performed to better understand the influence exerted by the change in the rotational velocity of a crystal and/or a crucible on the motion and thermal state of a liquid. We recall that these calculations were carried out for a higher value of the Rayleigh number (see Table 1).

In variant 3, the central body is stopped (in the rotating coordinate systems this corresponds to the rotation of the central body in the opposite direction with angular velocity Ω_C); all the remaining parameters correspond to variant 2. The instantaneous velocity distribution in the vertical section for this case is illustrated in Fig. 3c. A comparison of the velocity-vector field and the field depicted in Fig. 3b shows that the flow pattern has changed substantially, especially in the subcrystal region: the flow is more complex in the case of the rotating crystal. Figure 4c shows the distribution of the vertical velocity in the horizontal section. It is seen that strongly twisted spiral vortices whose system precesses in the direction opposite to the rotation of the vessel develop in the flow. On the whole, in the case of the stopped crystal the flow pattern demonstrates a more ordered form. We also note that the degree of deviation of the temperature distribution from axial symmetry is approximately the same for the cases of the rotating crystal and the stopped crystal, while the level of temperature pulsations in the subcrystal region is somewhat lower in the second case (Fig. 5c).

The curve of evolution of the temperature at the monitoring point shown in Fig. 5c also points to the more ordered flow in the absence of rotation of the crystal. The pronounced principal maximum is located at approximately the same frequency ($f \approx 0.1$–0.2) in the two variants compared. At the same time, the high-frequency spectral region is substantially more filled in the case of the rotating crystal (Fig. 5b). Certain differences also manifest themselves in the region of low frequencies. In Fig. 5c, less pronounced is the low-frequency modulation with a frequency of less than 10^{-2}, which is characteristic of the case of the rotating crystal. At the same time, the modulation with a frequency of $f \approx 0.02$ is pronounced in the case of the stopped crystal. On the whole, we can note that the opposite (in the fixed coordinate system) rotation of the crystal exerts a destabilizing influence on the flow, especially in the central part of the vessel.

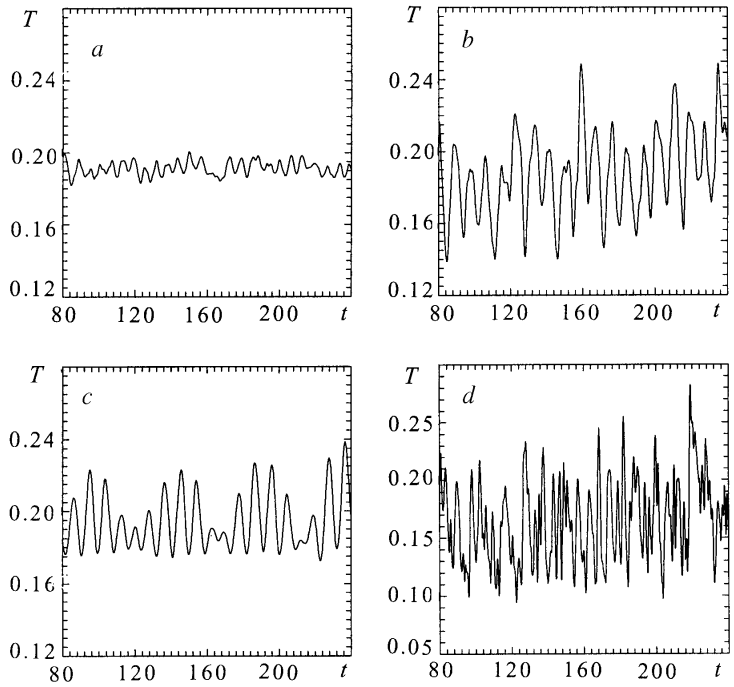

Fig. 5. Temperature fluctuations at the point $r = 0.1$, $z = 0.9$: a–d) variants 1–4 respectively.

By comparing variants 2 and 4 one can reveal the role of the Coriolis force. We note that a value of the Rossby number of 6.67 for variant 4 approximately corresponds to the upper limit of the range which is characteristic of the technology of crystal growth by the Czochralski method, whereas the value taken in variants 1–3 refers to the lower limit.

The increase in the Rossby number (attenuation of the Coriolis effects) leads to a sharp intensification of the flow. In particular, this is demonstrated by the instantaneous velocity distribution in the vertical section given in Fig. 3d. It is seen that a pronounced basic toroidal vortex is formed at the periphery of the vessel and weak secondary vortices are present at the sites of junction of the crucible walls with the free surface. The flow in the subcrystal region has a very complex structure: intense ascending and descending jets of the melt vibrating from side to side appear and disappear.

Figure 4d shows the instantaneous distribution of the vertical velocity in the horizontal section. The ascending flow predominates in the vicinity of the axis of rotation where flow is extremely intense. The value of the velocity nearly attains, from time to time, the value of the characteristic velocity of buoyancy. The vertical-velocity distribution gives no way of revealing the existence of any ordered structures. At the same time, the temperature distributions (they are not given) make it possible to judge the presence of the prevailing vortex structure with a wave number of $m = 3$. The system of three vortices, changing its appearance constantly, precesses in the direction opposite to the rotation of the vessel.

The graph of evolution of the temperature at the monitoring point (Fig. 5d) and the corresponding energy spectrum (Fig. 6d) point to the predominantly chaotic character of flow. A comparison of Fig. 6d and 6a–c shows that in the case in question the spectrum is substantially more filled. The spectral density of the signal in the region of high frequencies decreases with a rate of f^{-4}, which makes it possible to tentatively speak of the onset of the regime of "soft" turbulence [9].

6. The data given above demonstrate the development of intense large-scale vortices of three-dimensional pulsations in the subcrystal region and strong asymmetry of the instantaneous velocity and temperature fields. This is an important result in itself but it is also worthwhile to elucidate the influence of the three-dimensional self-oscillations of a melt on the averaged characteristics of flow, which can be done by comparing the results obtained for the same conditions in the three-dimensional and axisymmetric formulations.

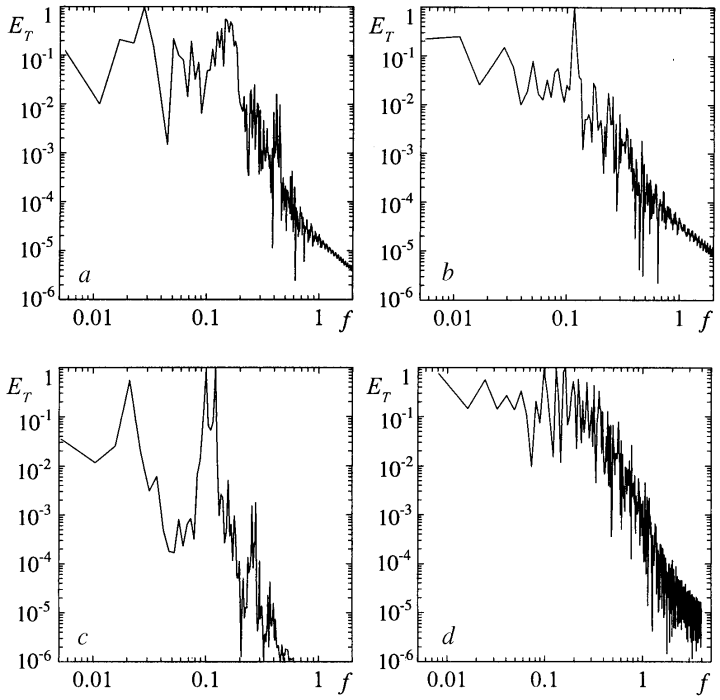

Fig. 6. Energy spectra of temperature fluctuations at the point $r = 0.1$, $z = 0.9$: a–d) variants 1–4 respectively.

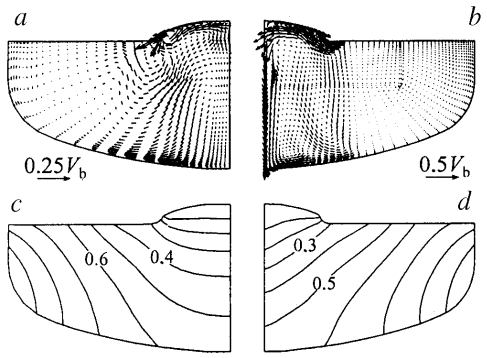

Fig. 7. Averaged velocity and temperature fields for variant 2: a and c) results of the calculation in the three-dimensional formulation; b and d) the same; in the axisymmetric formulation.

We calculated the unsteady convection in the axisymmetric formulation for the values of the diagnostic variables which correspond to variants 1–4 (see Table 1). Unlike the results described above and obtained in the three-dimensional formulation, the solution remained steady-state for variant 1 within the framework of the axisymmetric problem. The oscillations that occurred in regimes 2–4 were periodic and they were characterized by a much smaller amplitude of velocity and temperature pulsations than the amplitude obtained in the three-dimensional formulation.

Figure 7 shows the averaged velocity and temperature distributions in the vertical section obtained in the three-dimensional (a and c) and axisymmetric (b and d) formulations for variant 2. A comparison of the averaged velocity fields (Fig. 6a) and the instantaneous distributions (Fig. 3b) shows that the values of the averaged velocities are lower than the actual ones both in the subcrystal region and at the periphery of the flow. The distributions of the averaged temperature given in Fig. 7c demonstrate a strong radial equalization of the temperature in the subcrystal region; the isotherms are horizontal, in practice.

The structure of the flow calculated in the axisymmetric formulation (Fig. 7b) differs significantly from the structure given in Fig. 7a: the flow at the periphery is extremely weak, while in the subcrystal region the descending

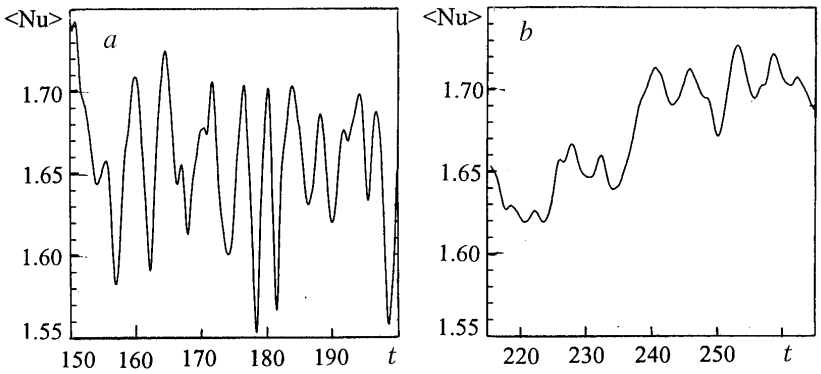

Fig. 8. Time evolution of the integral heat flux through the crystal/melt interface: a) variant 4 and b) variant 2.

flow predominates. The isotherms shown in Fig. 7d have a pronounced trough in the subcrystal region. Clearly, such a difference from the averaged temperature field which has been obtained in the three-dimensional formulation means a substantial radial nonuniformity of the heat flux supplied to the crystal, which can exert a strong influence on the prediction of the shape of the crystal/melt interface. Thus, for large Ra numbers the calculations in the axisymmetric formulation are in principle unable to correctly predict the temperature distributions in the subcrystal region.

An important characteristic which makes it possible to optimize the process of growth of a crystal is the quantity of heat supplied to the crystal/melt interface. The evolution of the integral heat flux through the interface with time is illustrated in Fig. 8 for two variants. It is seen that the three-dimensional pulsations exert a strong influence on the change in $\langle \mathrm{Nu} \rangle$ with time, especially for the case of weak rotation of the crucible: the pulsations of $\langle \mathrm{Nu} \rangle$ amount to 5–7% for $\mathrm{Ro} = 6.67$ (Fig. 8a). In the case $\mathrm{Ro} = 1.38$, we have a pronounced low-frequency component of the changes of the average heat flux (Fig. 8b). We can assume that the heat flux supplied to the interface and changing strongly with time creates conditions for the appearance of the fluctuations of the rate of growth of the crystal. The nonuniformity of the growth rate can lead to inhomogeneity of the properties of the crystal grown [1].

7. We have calculated the quasiperiodic and stochastic regimes of three-dimensional convection of a melt for the rotating vessel whose complicated shape is typical of crucibles which are used in growing crystals by the Czochralski method. It has been established that when the Rayleigh numbers are in the interval $10^4 - 10^5$ intense large-scale three-dimensional pulsations develop in the melt, predominantly in the subcrystal region; the counterrotation of the crystal destabilizes the flow of the melt, while the increase in the rotational velocity of the crucible, conversely, exerts a stabilizing influence. The values of the averaged velocities are substantially lower than the actual ones both in the subcrystal region and at the periphery of the flow. Three-dimensional pulsations lead to strong time changes of the integral heat flux which is supplied to the crystal/melt interface. The three-dimensional self-oscillations of the melt substantially change the statistically axisymmetric fields of velocity and temperature as compared to the fields obtained in the axisymmetric formulation and strongly decrease the radial nonuniformity of the heat flux supplied to the interface.

This work was carried out with support from the Russian Foundation for Basic Research under project 01-02-16697.

NOTATION

a, thermal-diffusivity coefficient; $\mathbf{e}_g$, unit vector in the direction of action of the gravity force; $\mathbf{e}_r$, unit vector in the direction of action of the centrifugal force; $\mathbf{e}_\Omega$, unit vector in the direction of the angular rotational velocity; E_T, density of the energy spectrum of temperature pulsations; f, frequency; t, time; g, acceleration of gravity; H, height; m, wave number; $\langle \mathrm{Nu} \rangle$, integral heat flux; p^*, modified pressure; $\mathrm{Pr} = \nu/a$, Prandtl number; R, radius; r, radial coordinate; $\mathrm{Ra} = (g\beta\Delta T H^3)/(\nu a)$, Rayleigh number in the gravity field; $\mathrm{Ra}_\Omega = (\Omega_c^2 \beta \Delta T R_c^4)/(\nu a)$, Rayleigh number in the centrifugal-force field; $\mathrm{Re} = (\Omega_s R_s^2)/\nu$, Reynolds number; $\mathrm{Ro} = V_b/(\Omega_c H)$, Rossby number; s, arc length along the crucible wall; T, normalized temperature; V, relative velocity; $V_b = (g\beta\Delta T H)^{1/2}$, velocity of buoyancy; z, vertical co-

ordinate; β, temperature coefficient of expansion; ΔT, scale of change of the temperature; ν, kinematic coefficient of viscosity; Ω, angular velocity. Subscripts: b, buoyancy; c, crucible; m, meniscus; s, crystal.

REFERENCES

1. G. Müller, *Convection and Inhomogeneities in Crystal Growth from the Melt*, in: H. C. Freyhardt (ed.), *Crystals*, Vol. 12, Springer-Verlag, Berlin–Heidelberg (1988).
2. A. Seidl, G. Müller, E. Dornberger, et al., *Electrochem. Soc. Proc.*, **98**, No. 1, 417–428 (1998).
3. S. Nakamura, M. Eguchi, T. Azami, et al., *J. Cryst. Growth*, **207**, 55–61 (1999).
4. M. Watanabe, M. Eguchi, K. Kakimoto, et al., *J. Cryst. Growth*, **151**, 285–290 (1995).
5. B. Basu, S. Enger, M. Breuer, et al., *J. Cryst. Growth*, **219**, 123–143 (2000).
6. C. Wagner and R. Friedrich, *Notes Num. Fluid Mech.* (Vieweg), **60**, 367–380 (1997).
7. N. V. Nikitin and V. I. Polezhaev, *Izv. Ross. Akad. Nauk, Mekh. Zhidk. Gaza*, No. 6, 81–90 (1999).
8. B. P. Leonard, *Comput. Meth. Appl. Mech. Eng.*, **19**, 59–98 (1979).
9. S. Togawa, S. Chung, S. Kawanishi, et al., *J. Cryst. Growth*, **160**, 41–48 (1996).